Shock Load Capacity of Concrete Expansion Anchoring Systems in Uncracked Concrete

H. Salim, M.ASCE[1]; R. Dinan[2]; J. Shull[3]; and P. T. Townsend, M.ASCE[4]

Abstract: Concrete anchoring systems are commonly used in blast resistant wall systems. These anchoring systems are often subjected to large tensile forces in a short time during an external blast event. Previous research has been conducted on anchoring systems to evaluate their response to cyclic and "shock" loads; however, the ultimate capacities of these systems were not determined, and tests were conducted at relatively slow loading rates. In this paper, testing has been performed to determine the ultimate capacity of various expansion anchors at high loading rates, which is characteristic of most blast events. Ultimately, concrete expansion anchors perform differently at high loading rates and some show improved ultimate performance. This paper will present the experimental findings and provide recommendations for anchor design under blast loads.

DOI: 10.1061/(ASCE)0733-9445(2005)131:8(1206)

CE Database subject headings: Blast loads; Bearing capacity; Cracking; Concrete; Anchoring.

Introduction

Terrorism is an increasing threat to many high profile government and commercial buildings. Most often, these structures are subjected to vehicle bombs that overwhelm the typical conventional constructed wall and window systems causing debris to enter the interior of the building, injuring personnel. Many of these structures are concrete frame buildings that utilize in-fill wall systems; therefore, engineers have been developing ductile cost efficient wall systems that provide protection for occupants of these facilities. Elastomer-reinforced concrete masonry unit walls, fabric reinforced masonry walls, and newly developed blast resistant steel-stud wall systems (Dinan et al. 2003) have all shown promise in providing acceptable protection. Many of these systems, such as the steel-stud wall, must be anchored to the concrete ceiling and floor slabs of the building using concrete anchoring systems. Postinstalled concrete anchoring systems are widely used because of their installation ease and variable placement in retrofitted facilities and new structures.

Most energy absorbent wall systems utilize tension membrane strength to be effective (Dinan et al. 2003). Steel-stud walls that are built using conventional construction techniques are relatively weak; however, if the steel studs are anchored properly, one can utilize the tensile capacity to create a highly effective blast remediation system. A stud loaded laterally, idealized as a flexible cable, creates tensile forces equivalent to the least cross section of the stud multiplied by the strength of the stud in question (Young 1989). Since the vertical anchorage forces govern the loading of the anchorage system, their tensile capacity is a major concern to the designer.

The static tensile strength of concrete anchors has been well defined by many, but the response of these systems to dynamic loads has not. The concrete capacity design (CCD) method, originally developed by Fuchs et al. (1995) and recently presented in ACI 318-02, Appendix D (ACI 2002), is widely accepted as the preferred method for computing the strength of fasteners loaded statically in tension and/or shear. The dynamic behavior of anchoring systems has been studied in depth by Collins at al. (1989) but has recently been presented for shock and cyclic loading situations by Hunziker (1999) and Rodriguez et al. (2001), respectively.

Hunziker (1999) studied the effects of shock loadings on concrete anchors installed in cracked concrete. He found that torque controlled expansion anchors often perform better in shock loading situations because of their ability for the expansion mechanism to reengage the concrete after initial movement. The amount of movement before engagement is dependent on load, but the ultimate strength showed increases of up to four times the static capacity of the anchor. Over 100 anchors were tested in cracked systems with given time to maximum load or rise times of approximately 80 ms. The study focused on the anchors' displacement behavior subjected to impulse loads, only two of the 100 tests failed due to pullout; most often, the ultimate capacity of these systems was never found. From field explosion tests on cladded steel-stud systems (Dinan et al. 2003; DiPaolo et al. 2003), it has been observed that the rise time for the peak loading was about 35 ms corresponding to a midspan deflection of 101.6 mm (4 in.). Since tensile membrane forces are larger at smaller postbuckled deflections in a steel-stud system, and since the rise time of 80 ms used by Hunziker (1999) may be slower than expected in an actual blast, it is important to investigate the an-

[1]Assistant Professor, Dept. of Civil and Environmental Engineering, Univ. Missouri-Columbia, Columbia, MO 65211-2200.

[2]Senior Research Engineer, Air Force Research Laboratory, AFRL/MLQF, Tyndall Air Force Base, FL 32404.

[3]Structural Engineer, Black and Veatch Special Projects Corporation, Security Consulting and Design Services, 6601 College Blvd. (Q3), Overland Park, KS 66211.

[4]Research Structural Engineer, U.S. Army Corps of Engineers, Engineer Research and Development Center, Vicksburg, MS 39180.

Note. Associate Editor: Barry Thomas Rosson. Discussion open until January 1, 2006. Separate discussions must be submitted for individual papers. To extend the closing date by one month, a written request must be filed with the ASCE Managing Editor. The manuscript for this paper was submitted for review and possible publication on December 23, 2003; approved on May 3, 2004. This paper is part of the ***Journal of Structural Engineering***, Vol. 131, No. 8, August 1, 2005. ©ASCE, ISSN 0733-9445/2005/8-1206–1215/$25.00.

chorage behavior under very short durations. In addition, the tests conducted by Hunziker (1999) were on anchorage systems installed in precracked concrete, which might not always be representative of the actual field situation. The effect of cracked concrete significantly reduces the capacity of an anchoring system (Rodriguez et al. 2001). Since most of the anchored slabs will be uncracked in the initial blast event, anchor capacities may be overconservative.

Collins et al. (1989) studied the effects of impact, shock, or dynamic loads on various anchoring systems, including the Hilti HSL torque controlled expansion anchor. They found that the load-displacement behavior of the expansion anchor loaded dynamically and statically is relatively similar, and the dynamic strength of the system can be estimated by the same method as in static cases. Also, the stiffness of the system is slightly decreased when subjected to dynamic load, but the amount of slip was not greater than its static counterpart. The expansion anchors were subjected to triangular pulse loads with a rise time of 250 ms and magnitudes less than or equal to the yield strength of the anchor steel. The study did not investigate the ultimate capacity of the system when subjected to dynamic load and rise times typical in blast environments as discussed earlier.

Rodriguez et al. (2001) extensively studied the effects of cyclic loading on many types of anchoring systems installed in various concrete substrates. They found that for some expansion anchors more displacement was allowed at maximum load; however, the maximum capacity of the anchor did not increase appreciably with dynamic loading. They also found that torque-controlled expansion anchors can exhibit increased dynamic capacities of up to 23% in uncracked concrete. Ramp or triangular pulse loading was applied to the anchors with rise times of 100 ms. Again, rise times for these tests may be considered inadequate for shock-type loads. Load controlled tests were conducted on a closed loop machine where anchor failure mode, deflection, and resistance were all recorded.

The test results of Rodriguez et al. (2001) showed insight into anchor embedment depth and concrete substrate makeup and their effect on anchor capacity. First, as embedment of an anchoring system decreases, normalized tensile capacity increases. Deeper embedment depths theoretically yield higher tensile capacities, but due to the anchors increased chance of pullout or pullthrough, slipping occurs until the embedment allows a cone failure at shallower depths than initially installed. Second, the type of aggregate used in the concrete does not significantly affect the concrete anchor's ultimate capacity. When expansion anchors were tested in limestone and river gravel, anchors using limestone aggregate showed a strength increase of only 2%. Finally, the use of slab reinforcement has negligible effects on the load-displacement behavior of a concrete anchoring system. Of all the anchoring systems tested, reinforced systems were 3% stronger than their unreinforced counterparts. To have any affect on the load-displacement behavior of the anchoring system, reinforcement must lie within the breakout cone, be oriented parallel to the applied load, and be developed in the surrounding concrete.

Testing done in this study will focus on certain types of expansion concrete anchor systems that have showed promise in dynamic loading situations or that are commonly used in retrofit applications (Salim et al. 2003). The anchoring systems will be tested in unreinforced uncracked 34.5-MPa (5,000-psi) river aggregate concrete. Static and dynamic tensile tests will be conducted on each anchor, with peak response times reaching 5.3 ms, to characterize the anchoring system's ultimate performance in blast environments.

In this paper, the failure modes of postinstalled concrete anchor systems is first summarized followed by the experimental program and discussion of the test results. Conclusions, recommendations, and future work are also summarized in this paper.

Postinstalled Concrete Systems

Expansion Anchor Types

There are two basic types of heavy-duty postinstalled concrete expansion anchor systems; deformation controlled and torque controlled. Expansion anchors transfer load by friction through the application of lateral pressure to the concrete hole. A Deformation-controlled anchor's expansion action depends on the amount of anchor slip with respect to the concrete surrounding. Deformation-controlled anchors include wedge and drop-in anchors. A torque-controlled anchor's expansion action depends on slip, but also the initial torque applied to the anchor (Collins et al. 1989).

Failure Modes

Concrete anchor tensile performance is largely dependent on the type of failure mode that a structural connection experiences. There are five basic failure modes that are associated with concrete anchor connection tensile behavior that are recognized by the U.S. Nuclear Regulatory Commission [U.S. Regulatory Commission (NUREG) 1998], namely, steel failure, cone failure, pull-out failure, pull-through failure, and splitting failure. One common failure mode is steel failure. This typically occurs at deeper embedment depths where the gripping mechanism of the anchor is adequate but the cross section of the anchor shank is not. Steel failure is defined by the area of the least cross section multiplied by the ultimate strength of the steel shank. Dynamic effects on the ultimate strength of the steel material of the anchor will not be considered since it is assumed that concrete failure will occur before the ultimate capacity of the bolt is reached.

The most common failure mode typically associated with concrete anchors is cone failure. Cone failure occurs when a fracture plane propagates from the bearing edge of the concrete anchor gripping mechanism and proceeds to the concrete surface at an angle between 35 and 45°. The CCD method is the accepted method by ACI 318-02 (2002) for defining the ultimate strength of concrete anchor or group of anchors subjected to loading in tension and/or shear. The CCD method for anchors loaded in tension will be summarized later in the paper.

Cone failures typically occur at shallower embedment depths. If the concrete anchoring system does not fail in the steel or in a cone-type mode, often the anchor experiences pullout or pull-through type failures. Pull-out failure occurs when the gripping mechanism does not provide enough frictional resistance for a given load and the anchoring systems "pulls out" of the hole in its entirety. Partial pullout can occur initially in a given load situation until frictional resistance matches the applied load and a cone-type failure occurs at depths shallower than originally installed. Pullthough is typical of deeper embedded expansion anchors whose gripping mechanism, such as an expansion sleeve, remains in contact with the concrete substrate but the body of the anchor disengages from the sleeve due to a localized steel failure and the anchor releases, taking no more load.

Currently, there is no specific accepted method for calculating pull-out or pull-through failure. Lateral blowout and splitting fail-

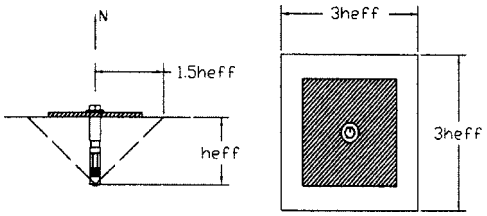

Fig. 1. Concrete capacity design method idealized failure plane and parameters

ure modes can occur but are much more infrequent. Lateral blowout failures occur when an anchor is placed near an edge where the embedment depth of the anchor is equal to, or less than, the edge distance. Large bearing stresses are introduced into the concrete from the anchor causing a conical mass of concrete to spall off the edge of the concrete substrate. The 45° method, presented in ACI 349 and summarized in Breen et al. (1995), and the CCD method both attempt to correct for edge effects where lateral blowout failures are a possibility; however, continuing research (Shull 2002) suggests that this approach is very conservative for large edge distances. Although further study needs to be done, it is suggested that Eq. (1) can be used to estimate the lateral blowout capacity in accordance with the 45° method

$$F_1 = Cm\sqrt{(A_b f'_c)} \tag{1}$$

where F_1=average lateral blowout capacity (N); C=constant =16.62; m=edge distance (mm); A_b=bearing area of anchor (mm)^2; and f'_c=concrete compressive strength (MPa).

Finally, splitting failures are cracks that form and propagate through a concrete plane, usually between a line or group of anchors. Splitting failures develop in situations when large expansion-force anchors are placed in weak concrete of compromising geometries, where the anchors are too close to the edge of a member, or installed in a thin member (NUREG 1998). Currently, there is no model that exists to predict splitting failures.

Concrete Capacity Design Method

The CCD method originally developed by Fuchs et al. (1995) and recently presented in ACI 318-02, Appendix D is widely accepted as the preferred method for computing the elastic behavior of ductile or nonductile fasteners subjected to tensile loadings, which fail along a concrete hypothetical plane as shown in Fig. 1. Eq. (2) defines the CCD method's tensile strength (ACI 2002)

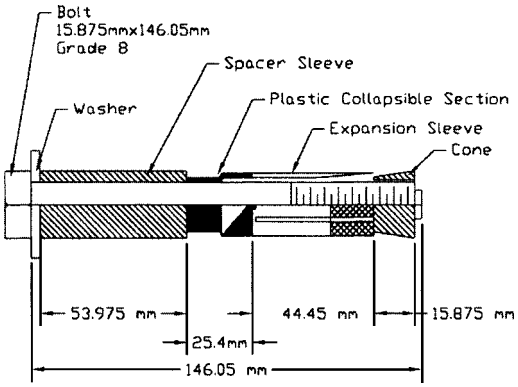

Fig. 3. Torque-controlled expansion anchor

$$N_{no} = K_{nc}\sqrt{f'_c}h_{\text{eff}}^{3/2} \tag{2}$$

where K_{nc}=14.66 for postinstalled anchors; and K_{nc}=16.75 for preinstalled anchors. N_{no} represents the tensile strength, in Newtons, of a postinstalled concrete anchor placed in concrete of compressive strength f'_c, in MPa, with an effective embedment depth of h_{eff} in mm. Eq. (2) is valid for a single concrete anchor placed in uncracked concrete, which is independent of edge influences including concrete boundaries and/or other anchorage devices. For anchors whose strength footprints overlap or infringe upon a concrete boundary, as in Fig. 2, Eq. (3) governs their performance. Eq. (3) represents the governing CCD edge effect strength reduction equation

$$N_n = \frac{A_n}{A_{no}}\psi_1\psi_2 N_{no}$$

$$\psi_1 = \frac{1}{1 + \dfrac{2e'_n}{3h_{\text{eff}}}} \leqslant 1; \tag{3}$$

$$\psi_2 = \begin{cases} 1.0 & \text{for} \quad C_1 \geqslant 1.5h_{\text{eff}} \\ 0.7 + 0.3\left(\dfrac{C_1}{1.5h_{\text{eff}}}\right) & \text{for} \quad C_1 \leqslant 1.5h_{\text{eff}} \end{cases}$$

where e'_n=distance between the resultant tensile load and the centroid of the fastener group (for a symmetric connection, ψ_1=1.0). Eq. (3) contains several correction factors including ψ_1, ψ_2, and A_n. ψ_1=tuning factor taking into account the connection between the centroid of anchor pattern and resultant tensile load.

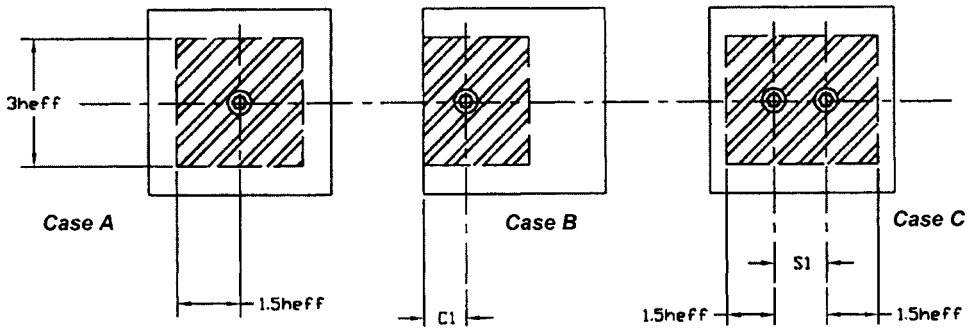

Fig. 2. Concrete capacity design method edge effect strength reduction cases

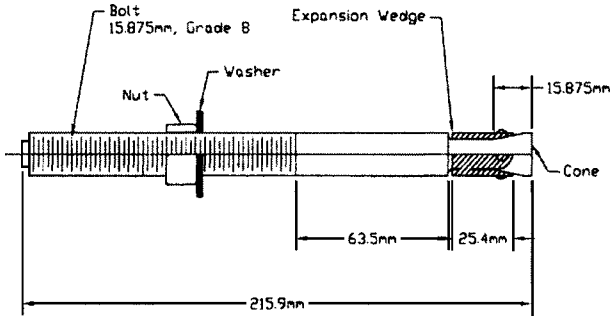

Fig. 4. Typical wedge anchor

ψ_2=tuning factor that accounts for the radial symmetric stress distribution of the connection. A_n=net area shown shaded in Fig 2. Edge effect strength reduction factors hinge on three main case criteria as shown in Fig. 2. For Case A, $A_{no}=A_n$, and for combination geometric cases containing Case B and C, strengths may be derived using similar logic.

In the following section, the shock load testing setup and description of each anchor system tested is provided. In addition, discussion of the tests results is presented.

Shock Load Testing

Test Specimens

Four different concrete anchor systems were selected for this study. The anchors were installed in a concrete anchor mount, described later, following manufacturer's recommendations. For all tests, once the hole was drilled, dust was blown from the hole using compressed air. Details of each anchor are presented next, followed by the test setup.

Torque Controlled Expansion Anchor
A 24-mm concrete hammer bit was used to drill a 152-mm deep hole in the concrete anchor mount. The 12.7-mm thick coupling device was placed on the mount then the anchor was placed in the hole and tightened to a specified torque of 204 N m. The Hilti HSL-16/25 torque-controlled expansion anchor (Hilti 2002), shown in Fig. 3, is comprised of carbon steel with an F_y=640 MPa and F_u=800 MPa.

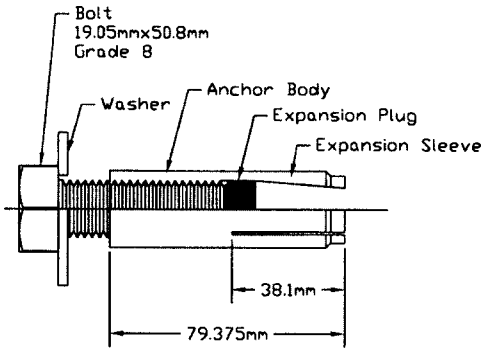

Fig. 5. Typical drop-in anchor

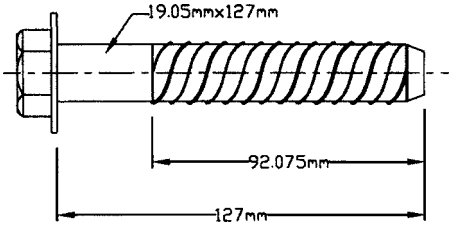

Fig. 6. Typical self-threading anchor

Wedge Anchor
A 15.9-mm concrete hammer bit was used to drill a 127-mm deep hole in the concrete anchor mount. After the anchor was driven into the hole, the coupling device was placed on the mount, then the anchor was tightened to a specified torque of 149 N m. The 16×178 mm Hilti KB II long thread wedge anchor, shown in Fig. 4, is comprised of carbon steel 8.8 with a yield capacity F_y=640 MPa and an ultimate capacity F_u=800 MPa.

Drop-In Anchor
A 25-mm concrete hammer bit was used to drill an 83-mm deep hole in the concrete anchor mount. The anchor body was placed in the hole, and a setting tool was used to drive the expansion plug through the expansion wedge until the setting tool shoulder met the top of the anchor. Once the plug was in the proper position, the 12.7-mm thick coupling device was placed on the mount then the bolt was threaded into the anchor and tightened to a specified torque of 109 N m (80 ft lbs). The Hilti HDI 19-mm drop-in anchor, shown in Fig. 5, is comprised of AISI

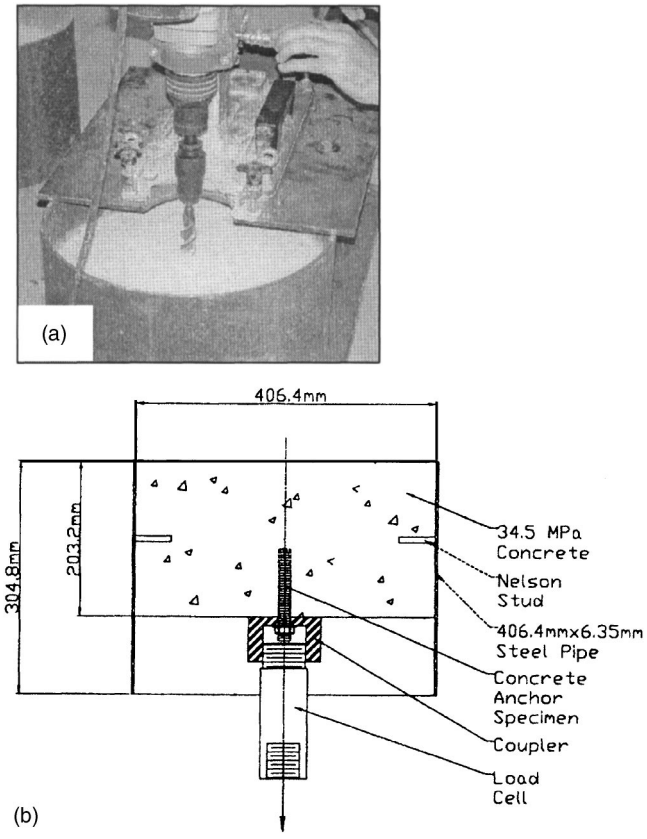

Fig. 7. Concrete anchor mount: (a) hole preparation; and (b) schematic test setup

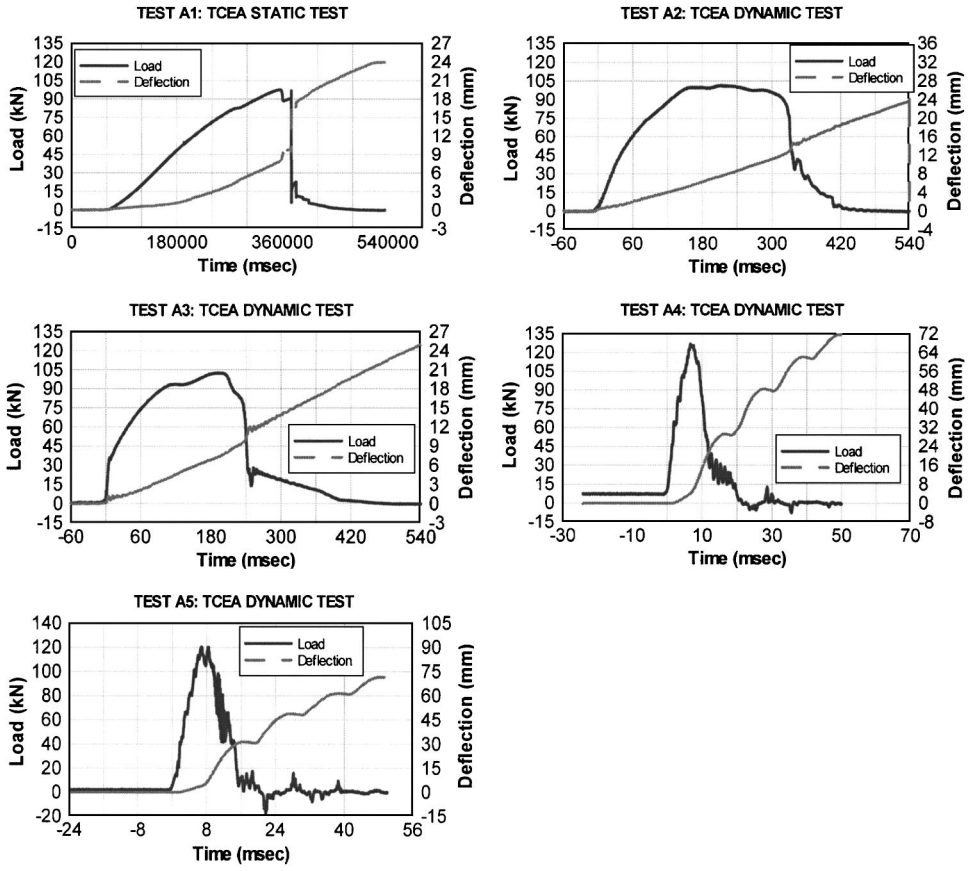

Fig. 8. Load and deflection time histories for torque-controlled expansion anchor Samples A1–A5

12L12 steel with a yield capacity F_y=414 MPa and an ultimate strength F_u=538 MPa.

Self-Threading Anchor

A 17.5-mm concrete hammer bit was used to drill a 127-mm deep hole in the concrete anchor mount. After the anchor was driven into the hole, the 12.7-mm thick coupling device was placed on the mount then the anchor was threaded into the hole and tightened with a maximum torque of 340 N m. The Powers wedge bolt, shown in Fig. 6 (Powers 2002), is comprised of AISI 1020 steel with a yield capacity F_y=295 MPa and ultimate strength F_u=395 MPa.

Test Setup

All concrete anchor specimens were installed in a concrete filled, steel pipe mount shown in Fig. 7. A steel pipe with a diameter of 406.4 mm and a wall thickness of 6.4 mm was cut into 305-mm sections then filled with 34.5±1.65 MPa-river aggregate concrete 203 mm above the mount base. To provide adequate shear resistance to hold the concrete in the pipe during loading, four 12.7-mm Nelson studs were welded to each mount 102 mm above the base at quarter points. Anchors were then installed at varying depths according to manufacturer's guidelines. To insure proper mounting of each anchor, a drilling stand was developed that allowed for the measurement of the drilling depth, placement of the anchor in the center of the mount, and perpendicular hole geometry.

The anchor mounts were attached to a coupling device, through a 445-kN tension link load cell attaching the specimen to the dynamic loading machine. The dynamic loading machine works by pressurizing cavities above and below a steel piston head with hydraulic fluid. Once the desired pressure is reached, a pneumatic valve is thrown and the pressurized hydraulic fluid below the piston head is released into an expansion tube; thus, forcing the piston downward. The rate at which the piston travels is dependent on the initial pressure of the cavities above and below the piston and the size of the pneumatic valve orifice. The machine has capacities in excess of 890 kN with variable loading rates of less than 5 ms of rise time. Deflection measurements were recorded using a cable-extension position transducer. All data were fed to a digital oscilloscope, saved, and later reduced and presented graphically as shown in Figs. 8–11.

Test Results

All four expansion anchors were tested to determine their ultimate capacities and failure modes when subject to varying loading rates. Complete load and deflection time histories are presented in Figs. 8–11 for each anchor test conducted, and the test results are given in Table 1, which summarizes the expansion anchor performance for each test conducted. Behavior of each anchor system is discussed next.

Torque Controlled Expansion Anchor

The torque-controlled expansion anchor (TCEA) system showed improved ultimate performance and increased stiffness as loading

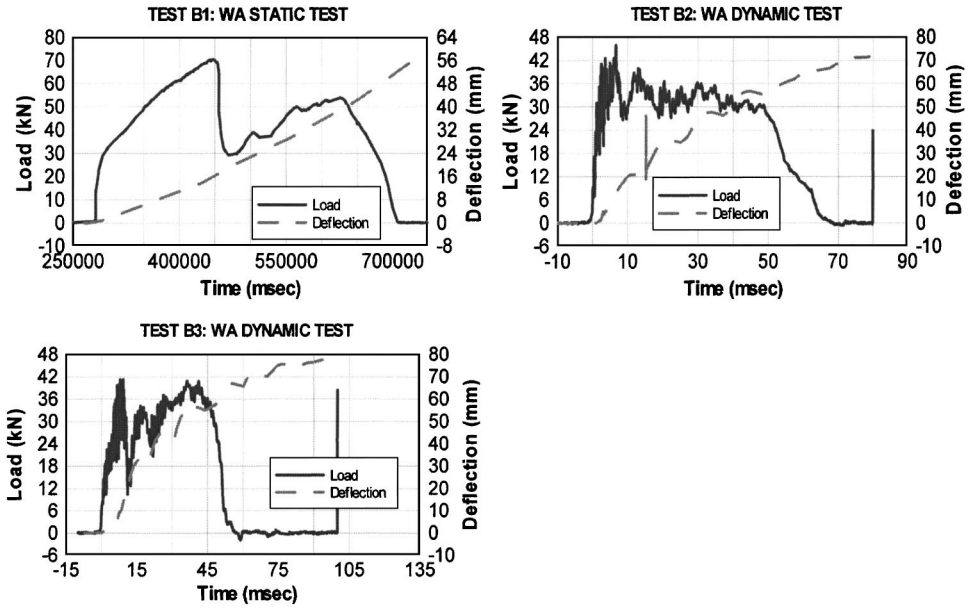

Fig. 9. Load and deflection time histories for wedge anchor Samples B1–B3

rates increased. Each anchor was tested in a similar manner and all exhibited a similar failure mode. Each anchor slipped initially until concrete failure occurred, which is visible in the load-deflection time histories by the sharp decrease in load following the fracture. The static strength of the anchor was slightly less than the predicted tensile strength using the CCD method and the initial embedment depths; however, if the deflection at failure is considered, the predicted ultimate tensile capacity is within 3% of the experimental value. As the loading rate increased, so did the ultimate tensile capacity. In Tests A4 and A5, the average dynamic capacity was 26% higher than that of their static counterpart. Also, the deflection at failure decreased as loading rates increased. Static Test A1 and Dynamic Tests A2 and A3 show similar deflections at failure, but Tests A4 and A5 experienced one-half of the deflection at failure; therefore, the stiffness of the system increased as loading rates increased. The load deflection curves for A1–A5 tests are shown in Fig. 8. The posttest pictures of the static test and two dynamic tests are shown in Fig. 12. In the static test, the concrete wedge remained intact, whereas in the dynamic tests the concrete wedge split at three or more locations. The higher loading rate resulted in more damage to the concrete wedge (Fig. 12). In addition, the overall diameter of the concrete wedge on the surface was larger for the dynamic tests than that for the static test (Fig. 12).

Wedge Anchor

The wedge anchor (WA) system showed decreased ultimate tensile performance and stiffness as loading rates increased. Like before, each anchor was tested in a similar manner, but failure modes between the static and dynamic cases are slightly dissimi-

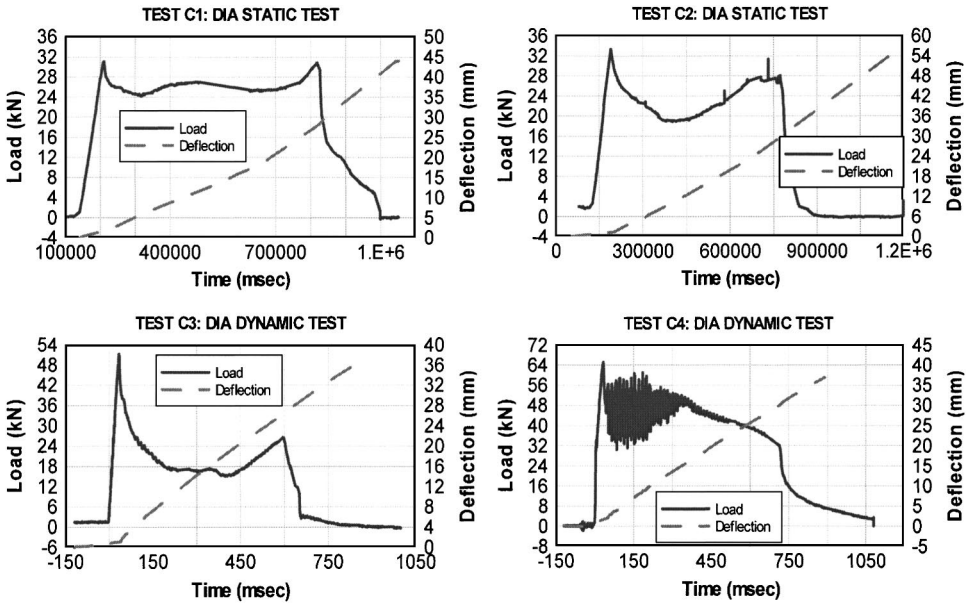

Fig. 10. Load and deflection time histories for drop-in anchor Samples C1–C4

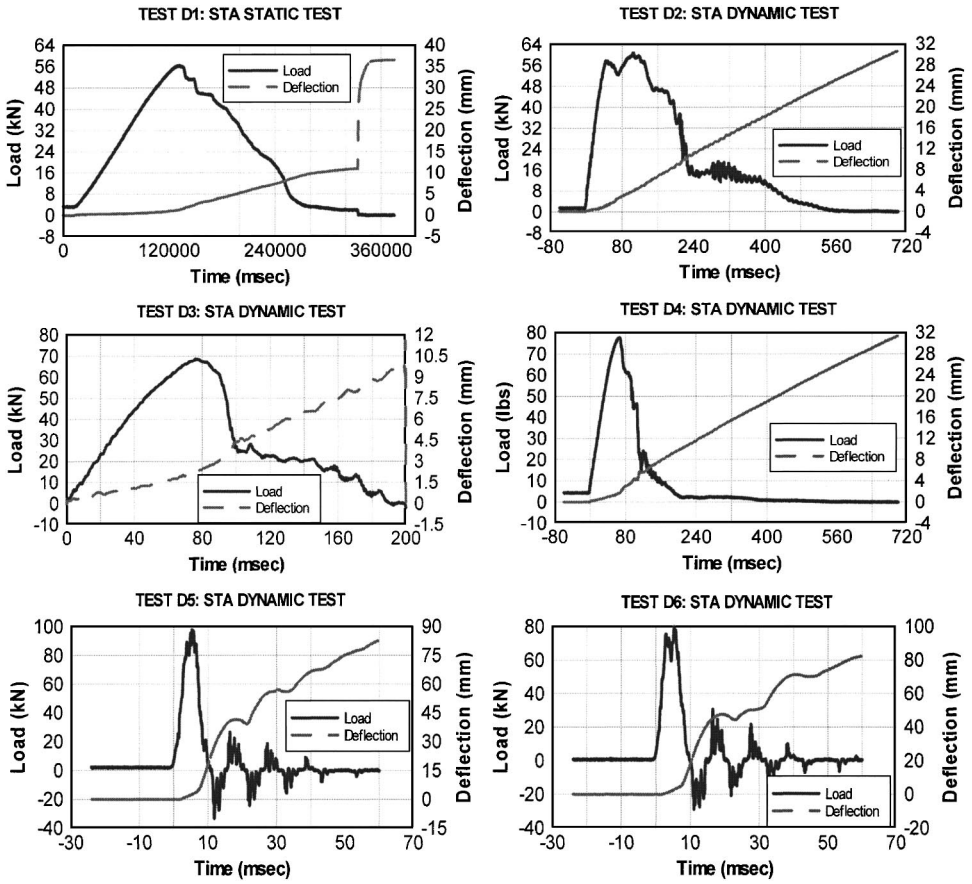

Fig. 11. Load and deflection time histories for self-threading anchor Samples D1–D6

lar. The statically tested anchor ultimately experienced a pull-though/pull-out failure. Maximum resistance occurred early in the load deflection time history, which preceded failure of the anchor system because the anchor continued to take load until the anchor disengaged at deflection in excess of 51 mm (2 in.). The concrete mount had visible cracks originating from the anchor hole that expanded radially outward. The failure mode explains the difference in tensile capacity between the CCD predicted strength and the experimental values.

Dynamically, the anchors initially experienced the same partial pull-through/pull-out behavior but concrete fracture caused failure. Concrete fracture did not occur in either dynamic case at the maximum tensile resistance, rather the anchor continued to take load until deflection reached more than 66 mm (2.6 in.), like that of the static case. Each dynamically loaded anchor showed less initial deflection but more ultimate deflection; however, maximum resistance also decreased causing the initial stiffness to decrease slightly. The wedge anchor also experienced decreased maximum resistance as loading rate increased. The CCD method did not accurately predict the ultimate capacity because of the partial pull-out/pull-through event that occurred early in the load deflection time histories. Decreased ultimate capacities combined with the decreases in system stiffness are indications of a weak-gripping system when compared to the Hilti HSL TCEA.

Drop-In Anchor

The drop-in anchor (DIA) anchoring system initially behaved in a similar manner as the WA, but unlike the WA, maximum resistance and stiffness increased as loading rates increased. Statically, the DIA maximum resistance occurred early in the load deflection time histories. Load continued to be resisted as the anchoring system initially experienced partial pullout, but concrete fracture governed toward the end of the load deflection time history. Unlike the WA, the DIA initial stiffness increased, and maximum resistance increased following increases in loading rate. Although fracture at initial embedment depth did not occur, the CCD method did come close to predicting the strength of the system at the original embedment depth. The anchor showed signs of increased dynamic capability as its performance shifted from a ductile weak-gripping anchor to a stiffer well-engaged system with some ductility.

Self-Threading Anchor

The self-threading anchor (STA) anchoring system showed signs of improved performance under dynamic loads. Upon testing of the anchoring systems, concrete fracture was the visible sign of failure; however, concrete fracture had initiated from the mid-height of the threads. The anchor did generally decrease in stiffness, but deeper origins of the fracture plane—where visible—at increased loading rates. In the statically loaded case, the maximum resistance is visible by a peak in the load-time history. Load falls off at an aggressive pace until a jump in deflection occurs, presumably the fracture of the concrete substrate. Dynamically, all anchors exhibit similar load deflection time histories as in the statically loaded case, but with less of a sharp rise in deflection at failure. The anchor ultimate tensile capacity did increase as the loading rate increased, but ultimate tensile capacity was overesti-

Table 1. Expansion Anchor Performance Summary

		Calculated	Measured					Dynamic effects[b]		
Test	Anchor type	CCD strength[a] (kN)	Ultimate capacity (kN)	Deflection at ultimate (mm)	Rise time (ms)	Stiffness (kN/m)	Rate of loading (kN/s)	Stiffness ratio	Strength ratio	Ratio[d]
A1	TCEA	105.13	97.70	7.87	Static	12,407.33	Static	1	1	0.97
A2	TCEA	105.13	101.72	7.62	213.0	13,349.42	477.5707	1.07593	1.041223	0.97
A3	TCEA	105.13	102.71	7.37	193.0	13,943.86	532.1785	1.12384	1.051335	0.98
A4	TCEA	105.13	127.09	4.06	6.6	31,271.54	19,255.69	2.520409	1.300856	1.21
A5	TCEA	105.13	120.29	3.56	6.8	33,828.01	17,690.06	2.726454	1.231302	1.14
B1	WA	105.13	70.42	17.27	Static	4,076.934	Static	1	1	0.67
B2	WA	105.13	45.95	11.94	6.6	3,849.112	6,962.227	0.944119	0.652553	0.44
B3	WA	105.13	41.29	12.19	9.2	3,386.409	4,487.728	0.830626	0.586325	0.39
C1	DIA	57.23	31.07	2.29	Static	13,589.44	Static	1	1	0.54
C2	DIA	57.23	33.32	1.27	Static	26,237.48	Static	1	1	0.58
C3[c]	DIA	57.23	51.33	1.02	33.0	50,518.01	1,555.342	1.925414	1.540331	0.9
C4[c]	DIA	57.23	65.17	2.03	33.0	32,071.97	1,974.856	1.222372	1.955796	1.14
D1	STA	105.13	56.54	1.27	Static	44,517.52	Static	1	1	0.54
D2	STA	105.13	60.73	4.06	105.0	14,944.29	578.4152	0.335695	1.074223	0.58
D3	STA	105.13	68.68	2.29	76.0	30,044.31	903.7013	0.674887	1.214797	0.65
D4	STA	105.13	77.75	1.78	67.0	43,726.63	1,160.387	0.982234	1.375128	0.74
D5	STA	105.13	97.96	2.54	5.4	3,8567.83	1,8141.17	0.866352	1.732704	0.93
D6	STA	105.13	79.84	2.79	5.3	2,8576.2	1,5064.51	0.641909	1.4122	0.76

Note: CCD=Concrete capacity design; TCEA=Torque-controlled expansion anchor; WA=Wedge anchor; DIA=Drop-in anchor; STA=Self-threading anchor.

[a]Based on initial embedment depth of 114 mm (4.5 in.) for TCEA, WA, and STA, and 76 mm (3.0 in.) for DIA. Concrete compressive strength =34.5 MPa (5,000 psi).

[b]Dynamic effects are calculated as a ratio of dynamic to static test result for each anchor group.

[c]Dynamic/static comparison made with static results for Test C2.

[d]Ratio of measured ultimate capacity to calculated strength using CCD method.

mated by the CCD method due to the anchors shallow fracture surfaces. The anchor consistently was stiffer than most other expansion systems but with ultimate tensile capacities lower than expected for large initial embedment depths.

Conclusions

TCEAs, WAs, DIAs, and STAs were tested in static and dynamic load situations indicative of shock loads that occur in blast events. All test results have only been validated for specific anchoring systems and loading rates defined above. The following conclusions can be summarized from the experimental data.

The Hilti HSL 16/25 TCEA ultimate tensile capacity and system stiffness will increase when the anchor is exposed to high dynamic loading rates and the CCD method will predict the static capacity within allowable limits. Upon dynamic load application, tensile capacity increased up to 21% above the CCD static prediction of tensile strength. The dynamically loaded system stiffness increased 2.7 times above the static case due to rises in tensile capacity and less initial deflection or slip.

The Hilti Kwik Bolt II WA ultimate tensile capacity and system stiffness will decrease when the anchor is exposed to high dynamic loading rates and the CCD method overestimates the static capacity of the anchor. Experimental ultimate tensile capacities were 67% of the CCD predicted strength. Upon dynamic load application, ultimate tensile capacity fell to 39% of the CCD predicted strength. Initial stiffness decreased when the loading rate increased; however, the ability of the anchoring system to provide resistance following the ultimate capacity yielded a somewhat ductile anchoring system.

The Hilti HDI DIA ultimate tensile capacity and system stiffness will increase when the anchor is exposed to high dynamic loading rates, but the CCD method will underestimate faster dynamically loaded systems. When exposed to dynamic loads, the DIA anchoring system will engage at a deeper depth than static cases, yielding tensile capacity increases of up to 14% above the CCD predicted strength.

The Powers wedge bolt STA ultimate tensile capacity increases as loading rate increases, but the CCD method ultimately overestimates the tensile strength of the system. Statically, the anchoring system exhibits poor performance when compared to CCD predicted values. Under dynamic load application, ultimate performance increases but only to 93% of the CCD predicted value.

Recommendations

It is suggested that the designer should consider using TCEA or an equivalent system because of its ease of installation, predictive static performance, and consistent improved dynamic capability in environments where tension shock loads are of high probable.

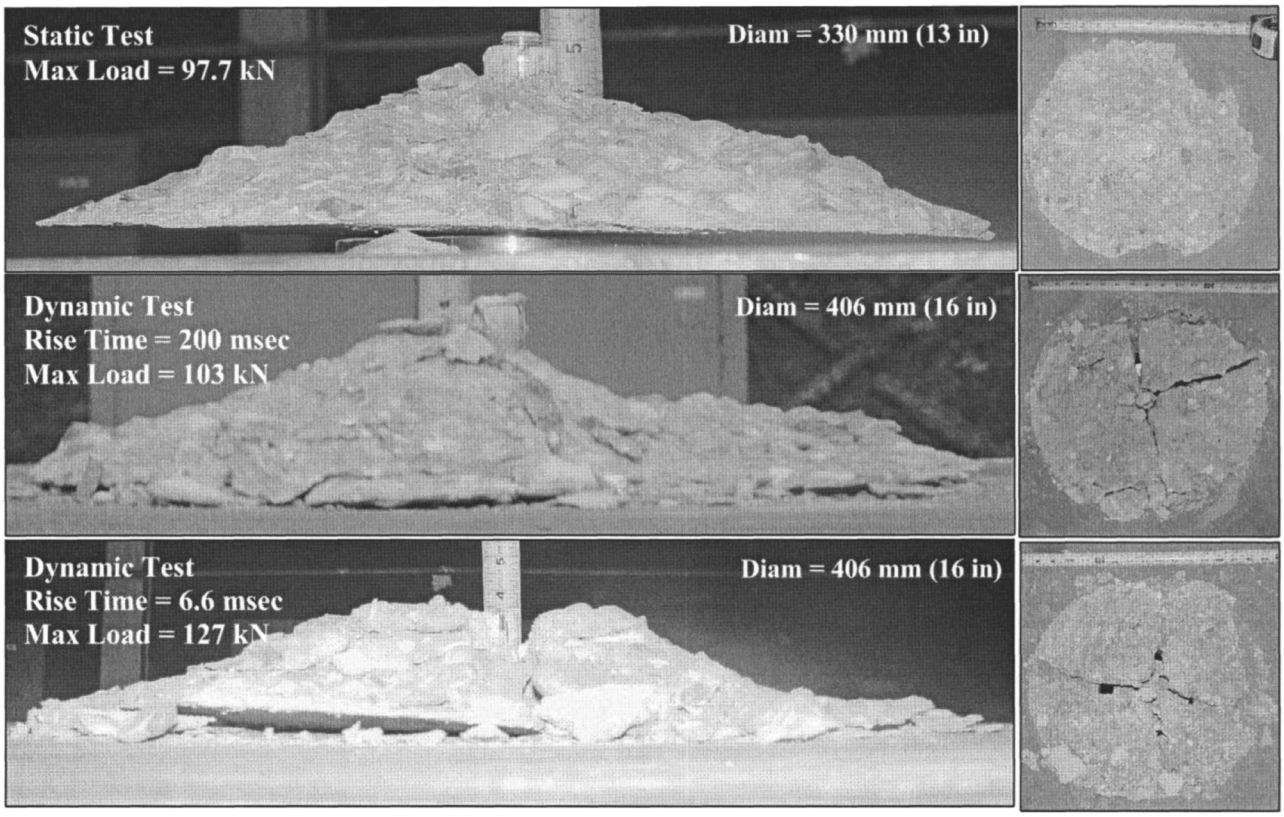

Fig. 12. Typical static and dynamic response of torque-controlled expansion anchor HSL-16/25 anchor

Limited testing on epoxy-based concrete anchoring systems have been performed. Epoxy anchoring systems are more economical than other anchoring systems due to their installation ease and low raw material costs. Since these anchoring systems transfer load in a different manner than expansion anchors, more testing is required to accurately predict the performance of these systems (Shull 2002).

Acknowledgments

The writers would like to acknowledge the research sponsorship of the U.S. Department of State (Mr. Wayne Ashbery, Mr. Donald Moffett) and the collaboration of the U.S. Army Corps of Engineers, Engineer Research and Development Center (Dr. Stanley Woodson and Dr. Beverly DiPaolo). Finally, the writers thank the Chief of Engineers for permission to publish this paper.

Notation

The following symbols are used in this paper:

A_b = bearing area of anchor;
A_n = projected area of concrete wedge;
C = constant;
e'_n = distance between the resultant tensile load and the centroid of the fastener;
F_1 = average lateral blowout capacity;
F_y = yield strength of anchor;
F_u = ultimate strength of anchor;
f'_c = concrete compressive strength;
h_{eff} = effective embedment depth;
K_{nc} = constant;
m = edge distance;
N_{no} = tensile strength of a postinstalled concrete anchor placed in concrete;
ψ_1 = correction factor; and
ψ_2 = correction factor.

References

American Concrete Institute (ACI). (2002). "Building code requirements for structural concrete (*ACI 318-02*) and commentary (*ACI 318R-02*)." Farmington Hills, Mich.

Collins, D. M., Klingner, R. E., and Polyzois, D. (1989). "Load-deflection behavior of cast-in-place and retrofit concrete anchors subjected to static, fatigue, and impact tensile loads." *Research Rep. No. 1126-1*, Center for Transportation Research

Dinan, R, Salim, H., Ashbery, W., Lane, J. and Townsend, P. T. (2003). "Recent experience using steel studs to construct blast resistant walls in reinforced concrete buildings." *Proc., 11th Int. Symp. on Interaction of the Effects of Munitions with Structures (11th ISIEMS)*, Streitkrafteamt, Germany and Defense Threat Reduction Agency.

DiPaolo, B., Salim, H., Townsend, T., and Davis, J. (2003). "A study on static and dynamic responses of exterior cold-formed steel-stud framing walls for enhanced blast resistance." *Proc. 16th Engineering Mechanics Conf.*, ASCE, Reston, Va.

Fuchs, W., Eligehausen, R., and Breen, J. E., (1995). Concrete capacity design approach for fastening to concrete." *ACI Struct. J.*, 92(1), 73–94.

Hilti (2002). *Systems and solutions customer catalogue* (brochure), Tulsa, Okla.

Hunziker, P. (1999). "Shock testing of concrete anchor bolts for shock

resistant applications in protective structures." *Proc. 3rd Int. Conf. on Shock and Impact Loads on Structures*,

Powers Faster Customer Catalogue. (2002) *Concrete anchor product information and availability* ⟨http://www.powers.com⟩

Rodriguez, M. et al. (2001). "Dynamic behavior of tensile anchors to concrete." *ACI Struct. J.*, 98(4), 511–524.

Salim, H., Dinan, R., Kiger, S., Townsend, P. T., and Shull, J. (2003). "Blast-retrofit wall systems using cold-formed steel studs." *Proc., 16th Engineering Mechanics Conf.*, ASCE, Reston, Va.

Shull, J. S. (2002) "Steel-stud retrofit connection development and design." MS thesis, Univ. of Missouri, Columbia, Mo.

U.S. Nuclear Regulatory Commission. (NUREG). (1998). "Anchor bolt behavior and strength during earthquakes." *NUREG/CR-5434*,

Young, W. C. (1989). *Roark's formulas for stress and strain*, 6th Ed., McGraw-Hill, New York.